Risky future for Mediterranean forests unless they undergo extreme carbon fertilization

Guillermo Gea-Izquierdo, Antoine Nicault, Giovanna Battipaglia, Isabel Dorado-Liñán, Emilia Gutiérrez, Montserrat Ribas, Joel Guiot

Risky future for Mediterranean forests unless they undergo extreme carbon fertilization

Running head: Mediterranean forests, climate change and CO_2

[1]G Gea-Izquierdo, [2]A Nicault, [3,4]G Battipaglia, [1]I Dorado-Liñán, [5]E, Gutiérrez, [5]M Ribas, [6]J Guiot

[1,7]INIA-CIFOR. Ctra. La Coruña km. 7.5 28040 Madrid, Spain. [2]Aix-Marseille Université/CNRS FR 3098 ECCOREV 13545 Aix-en-Provence, France. [3]Department of Environmental, Biological and Pharmaceutical Sciences and Technologies, Second University of Naples, Via Vivaldi, 43 - 81100 Caserta, Italy. [4]Ecole Pratique des Hautes Etudes (PALECO EPHE), Institut des Sciences de l'Evolution, University of Montpellier 2, F-34090 Montpellier, France. [5]Departament [4]Departament d'Ecologia, Universitat de Barcelona, Avda. Diagonal 643, 08028 Barcelona, Spain. [6]Aix-Marseille Université/CNRS/IRD UM 34, CEREGE 13545 Aix-en-Provence. [7]Corresponding author: phone 0034913471461; email gea.guillermo@inia.es

Abstract

Forest performance is challenged by climate change but higher atmospheric [CO_2] (c_a) could help trees mitigate the negative effect of enhanced water stress. Forest projections using data-assimilation with mechanistic models are a valuable tool to assess forest performance. Firstly, we used dendrochronological data from 12 Mediterranean tree species (6 conifers, 6 broadleaves) to calibrate a process-based vegetation model at 77 sites. Secondly, we conducted simulations of gross primary production (GPP) and radial growth using an ensemble of climate projections for the period 2010-2100 for the high-emission RCP8.5 and low-emission RCP2.6 scenarios. GPP and growth projections were simulated using climatic data from the two RCPs combined with: (i) expected c_a;

(ii) constant c_a = 390 ppm, to test a purely climate-driven performance excluding compensation from carbon fertilization. The model accurately mimicked the growth trends since the 1950s when, despite increasing c_a, enhanced evaporative demands precluded a global net positive effect on growth. Modeled annual growth and GPP showed similar long-term trends. Under RCP2.6 (i.e. temperatures below +2ºC with respect to preindustrial values) the forests showed resistance to future climate (as expressed by non-negative trends in growth and GPP) except for some coniferous sites. Using exponentially growing c_a and climate as from RCP8.5, carbon fertilization overrode the negative effect of the highly constraining climatic conditions under that scenario. This effect was particularly evident above 500 ppm (which is already over +2ºC), which seems unrealistic and likely reflects model miss-performance at high c_a above the calibration range. Thus, forest projections under RCP8.5 preventing carbon fertilization displayed very negative forest performance at the regional scale. This suggests that most of western Mediterranean forests would successfully acclimate to the coldest climate change scenario but be vulnerable to a climate warmer than +2ºC unless the trees developed an exaggerated fertilization response to [CO_2].

Keywords: Dendroecology; process-based models; carbon fertilization; climate change; MAIDEN; water stress; forest dynamics.

Type of paper: Original research article

Introduction

Future climate will trigger changes in ecosystem functioning, including enhancement in forest vulnerability to water stress (Giorgi & Lionello 2008; van der Molen et al. 2011; Anderegg et al. 2015). Understanding how forests will respond to warmer conditions but under higher than present c_a is crucial to assess future forest performance. Theoretically, plants should enhance growth and net primary productivity (NPP) by optimization of different functional traits in response to elevated [CO_2] (i.e. c_a levels way above present values, eCO_2) if this was a limiting factor. In practice, rising c_a has enhanced intrinsic water-use efficiency (iWUE) in forests but this was not generally translated on a net increase of growth, meaning that other factors such as water stress and/or nutrient limitation have overridden the potential positive effect of CO_2 (Peñuelas *et al*. 2011; Keenan *et al*. 2013; Reichstein *et al*. 2013; van der Sleen et al. 2014; Kim *et al*. 2016).

The net effect on tree growth of the interaction 'Climate x CO_2' can depend nonlinearly on c_a levels (Reichstein *et al*. 2013). Observational data show evidence up to current c_a < 403 ppm whereas future emission scenarios project c_a far above this level (IPCC 2014). Free-Air Carbon dioxide Enrichment (FACE) experiments were designed to address this issue. In these experiments [CO_2] was elevated up to 600-800 ppm but they were carried out under current environmental conditions mostly on temperate forests (Battipaglia *et al*. 2013; De Kauwe *et al*. 2013; Baig *et al*. 2015; Kim *et al*. 2016; Norby *et al*. 2016). Thus, the effect of eCO_2 on forest performance in relation to climate and other environmental factors needs to be addressed in other biomes where more constraining (warmer and drier) conditions are expected for the future (Giorgi & Lionello 2008; García-Ruiz *et al*. 2011; IPCC 2014). The role that CO_2 could play to compensate the negative impact of increasing water stress on forests has long been

debated. Plants can coordinate different functional traits in response to eCO_2 and drought-prone species at dry sites could benefit more from eCO_2 (Medlyn & De Kauwe 2013; Duursma *et al*. 2016; Kelly *et al*. 2016). Leaf-level responses are easier to predict than canopy or ecosystem-level responses (Fatichi et al. 2015). Consequently, there is still uncertainty on how the forest carbon cycle will adjust in the future because multiple interactive factors determine the net response of forests at different scales (Breda *et al*. 2006; Niinemets 2010; van der Molen *et al*. 2011; Kattge *et al*. 2011).

Vegetation models combine the effect of different stress factors on different functional traits to achieve a proper understanding of forest functioning. These models should be able to combine C-sink and C-source limitations to provide key information on how forests will develop in the future (Sala *et al*. 2012; McDowell *et al*. 2013; Fatichi *et al*. 2014; Anderegg *et al*. 2015; Walker *et al*. 2015). There is a constant need to improve the representation of hydrological, physical and biological processes in models. In addition, improvement of model performance needs to be achieved through benchmarking and data-assimilation (Peng *et al*. 2011; Pappas *et al*. 2013; Medlyn *et al*. 2015; Prentice *et al*. 2015). Dendrochronological data have long been used to assess empirical relationships between climate and growth, which can be used as an indicator of tree fitness and performance (Fritts 1976). Process-based models can take into account the influence of CO_2 on plant functional acclimation. Thus they can help to reduce uncertainty in growth projections but need continuous feedback from multiproxy data to ensure realism (Guiot *et al*. 2014; Walker *et al*. 2015). Dendrochronological records can be used to improve complex process-based models and help to assess forest dynamics under global change (Babst *et al*. 2014). Assessing forest dynamics is particularly challenging in ecosystems like those under Mediterranean climate (Morales *et al*. 2005) where two stress periods (cold in winter and drought in summer) limit plant

96 performance. Warmer winters could enlarge the growing season and promote higher
97 photosynthetic rates (just in evergreens) but also higher respiration rates, whereas
98 warmer summers would exert a negative impact (higher water stress) on forests.
99 Modeling the net effect on trees of the balance between these two periods is critical to
100 assess the future forest response to climate change.

101 We analyzed the effect that forthcoming changes in climate and c_a will yield over
102 Mediterranean forests, which are expected to face a high vulnerability to future climate
103 (Giorgi & Lionello 2008; García-Ruiz *et al*. 2011; IPCC 2014). We calibrated a stand
104 mechanistic model using a network of tree-ring growth chronologies including an
105 ensemble of species covering a wide ecological and geographic range to ensure realism
106 and biological robustness when simulating future forest performance at the regional
107 scale under different climate and c_a scenarios. C-assimilation and C-allocation were
108 explicitly controlled by climate and CO_2 at different phenological stages (Misson 2004;
109 Gea-Izquierdo *et al*. 2015). Importantly, the model includes a C storage pool to take into
110 account carry-over effects and its daily scale can fit different limiting environmental
111 conditions at different periods within and among years (Sala *et al*. 2012; Fatichi *et al*.
112 2014). Thus, the net effect in response to the winter and summer stress periods was
113 explicitly assessed. Forest projections were implemented using two contrasting
114 representative concentration pathways (RCPs, van Vuuren *et al*. 2011). Using model
115 simulations of future forest growth and GPP we addressed the following questions: (i)
116 what will be the net effect of a warmer climate for Mediterranean forests?; (ii) to what
117 extent could rising c_a help compensate the expected negative effect of climate warming
118 on forest growth and productivity? (iii) how will Mediterranean forests perform in
119 relation to the maximum temperature threshold for future climate (i.e. +2.0ºC respect to
120 preindustrial levels) agreed in the COP21 (http://www.cop21paris.org/)?

Material and Methods

Forest sites: growth data for model calibration

To calibrate the model at the regional scale we used dendrochronological data from 77 forest sites including 12 Mediterranean tree species: 6 conifers and 6 broadleaves (App. 1). These data were either owned by the authors or obtained from databases (ITRDB, https://www.ncdc.noaa.gov/data-access/paleoclimatology-data/datasets/tree-ring; DendroDB, https://dendrodb.eccorev.fr/framedb.htm). We explored the data to avoid chronologies where major site disturbances could have affected the decadal-to-multidecadal growth variations. The chronologies included were older than 80 years in order to avoid the effect of juvenile growth (data used for calibration started in 1950) and ended later than 1995. Exceptionally, some sites ending before 1995 in Algeria were included to ensure enough data from that region. The resulting calibration period slightly differed across sites due to the different time-span of chronologies, but always fell between 1950 and 2010 and was greater than 40 years. For the analysis, ring-width growth data were transformed to basal area increments (BAI, cm^2 $year^{-1}$). One output from the model is C allocated to the tree stem (g C m^{-2} $year^{-1}$). To make BAI and model output comparable for model calibration both data were normalized to unitless indices (Misson 2004; Gaucherel et al. 2008).

Climate and c_a: historical data and future scenarios

Daily precipitation and temperature data used for model calibration for 1950-2010 were either obtained from http://www.meteo.unican.es/datasets/spain02 (Herrera *et al.*, 2012) for Spain (20 km grid) or from http://hydrology.princeton.edu/data.php (Sheffield *et al*. 2006) for the rest (1º grid). Data were downscaled to match mean climatic local

values where these were available. For the future forest projections we used two greenhouse gas (GHG) radiative forcing scenarios developed for the Fifth Report of the IPCC (IPCC 2014), called RCPs (Van Vuuren *et al*. 2011). RCP8.5 (GHGRF<8.5 W/m^2) is the "business as usual" scenario. RCP2.6 is the most optimistic and stringent among RCPs, corresponding to strong mitigation policies with a GHG radiative forcing constrained to remain <2.6 W/m^2. RCP2.6 is the only RCP limiting global warming to +2°C relative to the pre-industrial level. We used a multimodel ensemble of 19 simulations for RCP2.6 and 18 simulations for RCP8.5 performed by 13 climatic institutes (see App. 2). The global climate models have a coarse resolution, from one to more than five degrees depending on the model. There is often some mismatch between the stand level and input climatic data (Körner 2003; Potter et al. 2013; Pappas et al. 2015). This was minimized as possible by downscaling climate scenarios to match the shared period of the historical data. Under RCP8.5 the projected climate for our study sites describes a relative increase in mean annual temperature (MAT) of +5.0ºC and a decrease of over 40% in mean annual precipitation (MAP) by 2100 respect to current values. Under RCP2.6 the projected climate forecasts a mean increase in MAT of +1.0ºC by 2068, stabilizing thereafter, with no decrease in MAP respect to current conditions (App. 3).

The process-based model MAIDEN

The vegetation model MAIDEN (Fig. 1) was originally developed to be used with dendrochronological data by being calibrated to both time series of radial growth and estimates of transpiration from sap-flow experiments (Misson 2004). Recently, the model has been further developed to be used with evergreen Mediterranean taxa with a multiproxy approach using gross primary productivity (GPP) estimates from Eddy

171 covariance stations and plot growth data (Gea-Izquierdo *et al*. 2015). Inputs are daily
172 climatic data (precipitation, maximum and minimum temperatures) and c_a. In addition

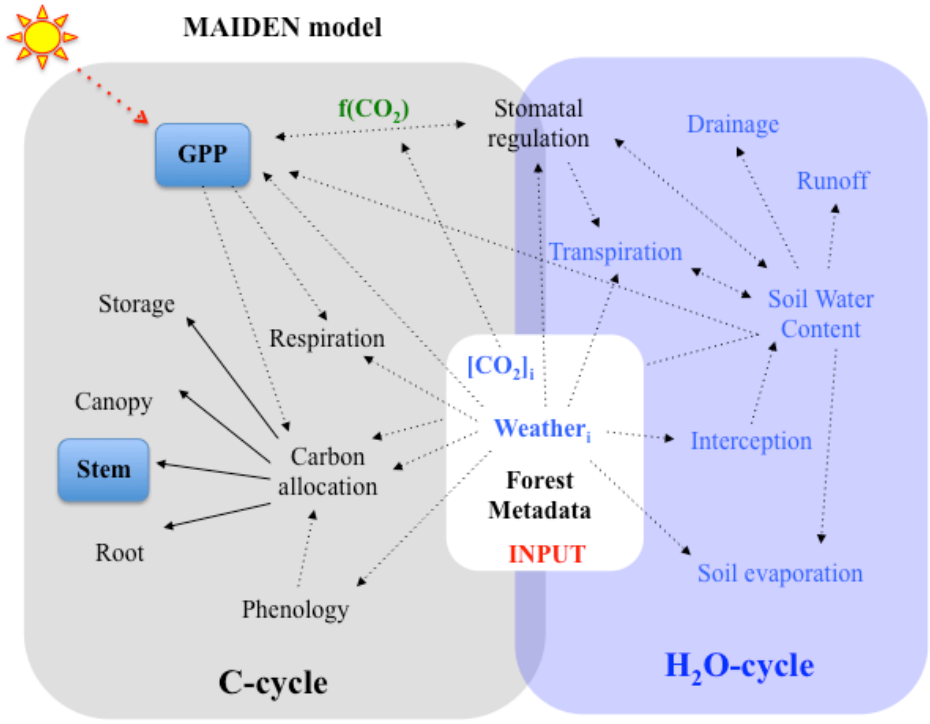

173
174 Fig. 1. Outline of MAIDEN. Only GPP (gross primary production) and biomass
175 allocated to the stem (used to calibrate the model sitewise) estimates (blue boxes) are
176 reported along the manuscript. Daily output of each variable is generated based on the
177 input data of day i. 'Weather' corresponds to daily integrals of precipitation as well as
178 maximum and minimum daily temperatures. GPP and 'Stomatal conductance' are
179 functions of CO_2, whereas variability within the other processes is mostly driven by
180 meteorological inputs directly or indirectly (e.g. SWC). For more details on the
181 functions and processes outlined see Misson (2004) and Gea-Izquierdo *et al*. (2015).
182
183 the model requires as input different site related physiographic characteristics and
184 species functional traits (see Gea-Izquierdo *et al*. 2015 for details). The processes within
185 the model are mainly functions of climate, CO_2 and soil water availability (hence water

186 stress). The model acts at the stand level calculating carbon and water fluxes (Fig. 1)
187 using a coupled photosynthesis-stomatal conductance model. It uses the standard
188 biochemical model of Farquhar *et al*. (1980) in which photosynthesis is driven by the
189 most limiting between Rubisco-limited activity and electron-transport. Stomatal
190 conductance is also estimated using a widely used equation as a function of vapor
191 pressure deficit (VPD, Leuning 1995). After GPP and autotrophic respiration have been
192 estimated carbon is allocated to different tree components. Photosynthesis and
193 allocation are driven by decoupled non-linear (daily) functions of climate. Thus growth
194 is not only a direct function of C availability and the model is designed to address in
195 time not only C-source but also C-sink limitations, which is an important step required
196 to achieve more robust and realistic vegetation models (Muller *et al*. 2011; Sala *et al*.
197 2012; Fatichi *et al*. 2014). The model is particularly sensitive to water stress by
198 implicitly modeling as functions of climate and water stress some functional and
199 demographic traits such as leaf area, carbon allocation, leaf- and canopy-level
200 photosynthesis and transpiration (Muller *et al*. 2011; Gea-Izquierdo *et al*. 2015;
201 Duursma et al. 2016; Kelly et al. 2016). [CO_2] only affects photosynthesis and stomatal
202 conductance, i.e. leaf area or respiration are direct functions of climate but not CO_2. A
203 brief outline of the model is shown in Fig. 1.
204
205 *Model calibration and ecological coherence of the parametric space*
206 Calibration of complex multiparametric models is necessary to improve model
207 performance and because of the presence of collinearities between parameters and
208 absence of an exact solution (Prentice *et al*. 2015). To ensure good model performance,
209 it is important to assess the functional coherence of parameters to be calibrated. In
210 addition to calibration, it is desirable to run independent validations particularly when

models are fitted for prediction purposes. Nevertheless, we could not run an independent crossvalidation for two reasons: (1) we calibrated against annual growth (i.e. we had a number of observations between 40 and 60) estimates by integrating annually the daily estimates from the model, therefore our data was too short to be split in two, (2) a jackknife was intractable both computationally and also because continuous (daily) time data series are needed to run the model, i.e. in case individual years were left out the model could not calculate the carbon and water dynamics needed to compute the complete time series at each site.

We implemented a species-specific approach rather than using plant functional types (PFTs) as it is often applied in ecosystem models (Kattge *et al*. 2011; Atkin *et al*. 2015; Pappas *et al*. 2016). We applied the model at the regional scale and to different species to analyze forest performance under future climate and c_a. Data-assimilation was used to apply the model to different ecological conditions and species (Peng *et al*. 2011; Medlyn *et al*. 2015). Overall, the growth data did not show a positive trend whereas c_a increased steadily in the calibration period (1951-2010). Therefore, by calibrating the model site-wise using non-detrended (but normalized) growth data and observed c_a levels we assured that the model excluded an artificial carbon fertilization effect on past growth. Additionally, to avoid overestimation of photosynthesis and get unbiased simulations (Schaefer *et al*. 2012), we ensured that maximum GPP daily integrals yielded within ranges given in Baldocchi *et al*. (2010): 4-6 g C m^{-2} day^{-1} for evergreens and of 10-14 g C m^{-2} day^{-1} for deciduous species. Similarly, we constrained annual GPP and NPP estimates to be within those measured for similar ecosystems (see Table 3 in Falge *et al*. 2002 and Table 3 in Luyssaert *et al*. 2007). Species Specific leaf area (SLA) was obtained from Mediavilla *et al*. (2008) and Kattge *et al*. (2011).

Here, within the processes in Fig. 1 we show those functions with parameters involved in the calibration phase. For more details, we refer to the original model in Misson (2004) and the updated modified last version in Gea-Izquierdo *et al*. (2015).

(i) $\theta_g(i) = \frac{1}{1+\exp(soil_b \cdot (SWC(i) - soil_{ip}))}$ [E1]

(ii) $a_{31}(\mathrm{i}) = (1 - \exp(p_{3moist} \cdot SWC(i)) \cdot \left(\exp\left(-0.5 \cdot \left(\frac{T_{max}(i) - p_{3temp}}{p_{3sd}}\right)^2\right)\right)$ [E2]

(iii) $a_{32}(\mathrm{i}) = (1 - \exp(st_{3moist} \cdot SWC(i)) \cdot \left(\exp\left(-0.5 \cdot \left(\frac{T_{max}(i) - st_{3temp}}{st_{3sd\_temp}}\right)^2\right)\right)$ [E3]

(iv) $a_4(\mathrm{i}) = \left(1 - \exp(st_{4temp} \cdot T_{max}(i)\right) \cdot \left(\exp\left(-0.5 \cdot \left(\frac{SWC(i)}{st_{4sd\_moist}}\right)^2\right)\right)$ [E4]

θ_g is a soil water stress function affecting stomatal conductance. a_{31}, a_{32} and a_4 are allocation functions for two different phenological periods (3 and 4). a_{31} is related to the leaves and a_{32} to the stem, whereas a_4 determines C allocation between the stem and storage. SWC is soil water content and T_{max} is daily maximum temperature. We calibrated $soil_{ip}$ from [E1]; p_{3moist} and p_{3temp} from [E2]; st_{3moist} and st_{3temp} from [E3]; and st_{4sd_moist} and st_{4temp} from [E4]. The rest of parameters were set following Gea-Izquierdo *et al*. (2015). All parameters except $soil_{ip}$ (which is related to the stomatal response) help to define carbon allocation in relation to soil water content and air temperature during the active period.

We calibrated these model parameters taking into account variability in functional traits and the response to climate of plant processes related to site and species. To address the local phenotypic response of species (Montwé *et al*. 2016), some of those parameters (≤7) described in the previous paragraph were calibrated site-wise using maximum likelihood principles and a global optimization algorithm (Gaucherel *et al*. 2008; Gea-Izquierdo *et al*. 2015). A maximum of 7 allocation parameters from [E1] to [E4] were optimized depending on species by comparing normalized annual integrals of

modeled C allocation to the stem and normalized annual growth series. We calculated different statistics to check the goodness of fit: the coefficient of determination (R^2), the linear correlation (ρ), and the correlation (r_{low}) between filtered (using splines with a 50% frequency cutoff of 30 years) observed and modelled growth. r_{low} was calculated to analyse the model capability to mimic the interannual and decadal growth trends. To discuss the validity of our modelling exercise and since we could not run an independent verification to the calibration conducted, coherence of the intersite multiparametric space was analysed by exploring the ecological significance of parameters compared to different site characteristics including latitude, longitude, altitude, precipitation, temperature, and Penman-Monteith potential evapotranspiration (PET), which was calculated for each site following Allen *et al*. (1998). The relationship between the 7 model parameters fitted at each of the 77 sites and the mean site ecological covariates was explored through pointwise correlations: (i) using site individual indices; (ii) using the principal components (PCs) of the 7 x 77 matrix (Legendre & Legendre 1998).

Forest performance under climate change and different c_a scenarios

Once the model had been calibrated we implemented forest projections at the 77 sites using simulated climatic data generated under RCP2.6 and RCP8.5. To discuss the effect of c_a on the net response of forests to climate change we compared two type of forest simulations driven by the multimodel climatic scenarios:

(i) 'fertilization' scenario: with c_a levels expected for RCP2.6 and RCP8.5.

(ii) 'non-fertilization' scenario: using climate from RCP2.6 and RCP8.5 but constant c_a = 390 ppm after 2010.

We report GPP in addition to growth projections. Future growth trends were assessed

Group	n	R^2		r		r_{low}	
		Mean (sd)	Max (Min)	Mean (sd)	Max (Min)	Mean (sd)	Max (Min)
Broadleaves	22	0.343 (0.168)	0.643 (0.0)	0.675 (0.084)	0.821 (0.483)	0.728 (0.185)	0.929 (0.114)
Conifers	55	0.356 (0.141)	0.710 (0.073)	0.676 (0.070)	0.855 (0.537)	0.786 (0.156)	0.968 (0.249)
Total	77	0.353 (0.148)	0.710 (0.0)	0.675 (0.074)	0.855 (0.483)	0.769 (0.165)	0.968 (0.114)

283 Table 1. Mean values of goodness of fit statistics. n= number of forest sites; R^2=coefficient of determination; r=coefficient of correlation;

284 r_{low}=coefficient of correlation of filtered data (see material and methods for details).

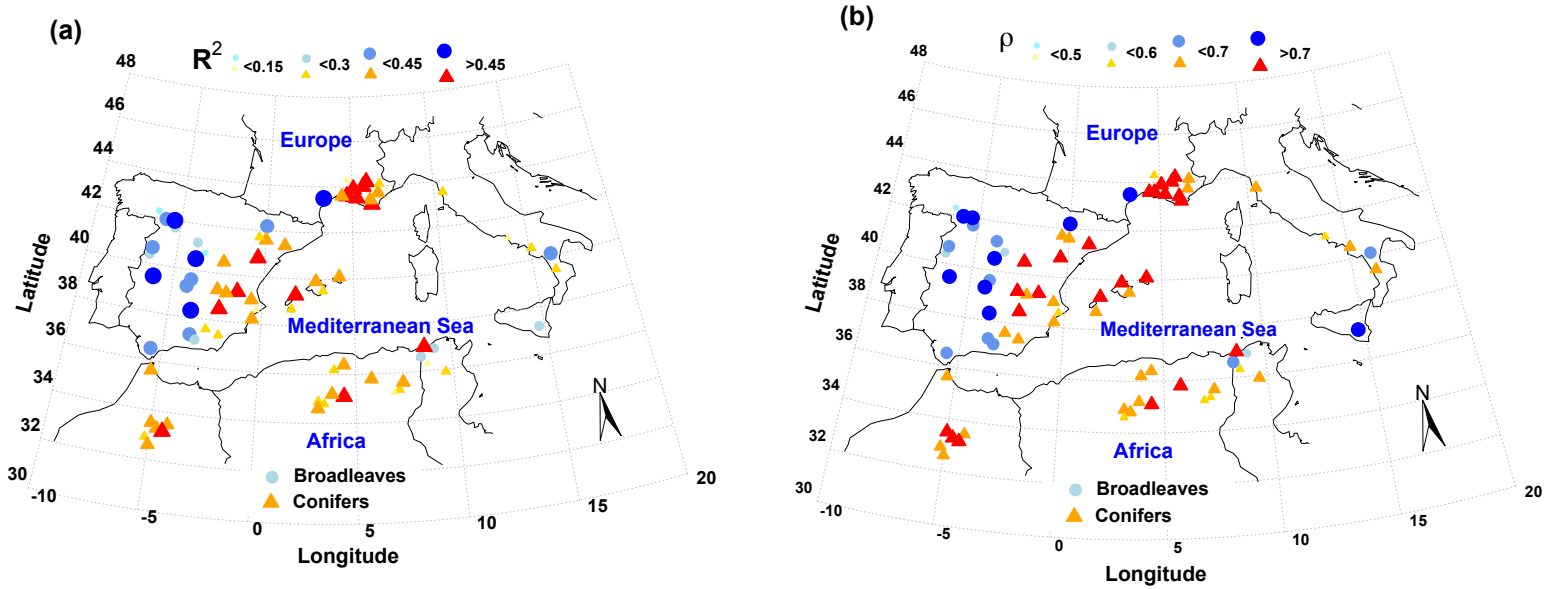

285

286 Fig. 2. Map showing the coefficient of determination (R^2) and correlation (ρ) between dendrochronological data and modeled stem growth data

287 using MAIDEN at the 77 forest sites. R^2 is shown in (a) whereas ρ in (b). For R^2 we split in four classes: $0 \leq R^2 < 0.15$; $0.15 \leq R^2 < 0.3$;

288 $0.3 \leq R^2 < 0.45$; $0.45 \leq R^2$. For ρ in: $0.45 \leq \rho < 0.5$; $0.5 \leq \rho < 0.6$; $0.6 \leq \rho < 0.7$; $0.7 \leq \rho$. Triangles depict conifers, whereas circles broadleaves.

289 through the slope of simple regressions between simulated growth (or GPP) for a given
290 scenario and site against year for the periods 2010-2100, 2010-2050 and 2051-2100.
291
292 **Results**
293 *Model calibration across western Mediterranean forests*
294 The model fit against the calibration data is shown in Fig. 2 and Table 1 and the
295 parameters fitted in App. 4. Importantly, data used to calibrate the model did not show
296 an overall significant increase in growth, hence did not suggest evidence of a global net
297 carbon fertilization effect during the last decades (Table 2). The observed growth trends
298 were highly correlated with the model output (ρ and particularly r_{low} in Table 1).
299 Correlation between model output (carbon allocated to the stem) and growth data was in
300 average 0.67 whereas mean R^2 was 0.36 (Table 1). The multiparametric space of the 77
301 fitted models was explored through PCA. The eigenvalues corresponding to the three
302 first principal components (PCs) were over the mean, hence significant according to the
303 Kaiser-Guttman criterion (Legendre & Legendre 1998). These three PCs including the 7
304 parameters fitted in the calibration phase explained 60.9 % of the variability (PC1 24.7
305 %, PC2 19.7 % and PC3 16.6%). PC1 was mostly related to parameters linked to
306 humidity: a positive relation with moisture parameters such as $soil_{ip}$ and st_{4sd_moist}, and
307 a negative one with st_{3moist} (not shown). PC2 was mostly related to parameters linked
308 to temperatures: positively with st_{4temp} and negatively with p_{3temp} and st_{3temp}. PC3
309 was positively correlated with the humidity parameter p_{3moist} (not shown). The 77
310 parameters and the PCs (2 and 3) showed some significant relationships with the site
311 ecological characteristics (Fig.3). Most of the site-based relationships between the fitted
312 parameters and the ecological characteristics of the 77 sites were linked to site
313 temperatures (Fig. 3), whereas almost no significant relationships were found with the

other tested covariates (e.g. site precipitation or PET). These relationships suggest the existence of some ecological coherence within the parametric space fitted for the 77 forest sites, which would support the robustness of the model parameterization used.

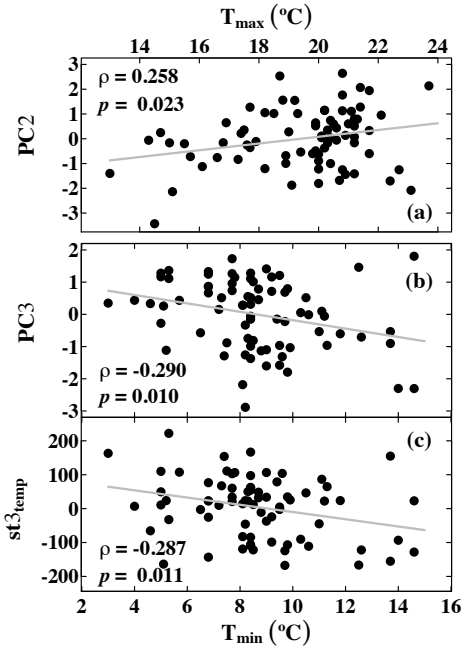

Fig. 3. Ecological coherence of model parameters at the 77 forest sites (only those relationships that were significant are shown): (a) PC2 and site T_{max}; (b) PC3 and site T_{min}; (c) $st3_{temp}$ and site T_{min}.

Growth-GPP projections under changing climate and c_a

The model allocates carbon to different plant compartments driven by different non-linear functions of environmental variability, hence it allows some decoupling between GPP, NPP and secondary growth. In this sense, 59% and 80% of the simulations presented correlations between GPP and growth higher than 0.5 for RCP2.6 and RCP8.5, respectively (App. 5). Thus the majority of sites showed a good agreement between interannual GPP and growth (i.e. generally the modeled interannual variability of growth was driven by that of GPP). Furthermore, the growth trends (long-term, multiannual) were of similar sign (positive, negative or neutral) as those of GPP (Table

Group	Observed past Growth		Growth projections 2010-2099							
			Allowing fertilization (i.e. predicted c_a)				No fertilization (i.e. c_a = 390 ppm)			
			GPP		Growth		GPP		Growth	
			2010-2050	2051-2099	2010-2050	2051-2099	2010-2050	2051-2099	2010-2050	2051-2099
Broadleaves	0.79 (0.96)	RCP2.6	0.60 c (2.03)	-0.62 c (0.38)	0.35 b (0.71)	-0.24 d (0.16)	-2.2 a (2.75)	0.26 a (0.47)	-0.65 b (0.89)	0.08 a (0.18)
Conifers	0.17 (0.71)		0.78 c (1.98)	-0.98 d (1.42)	0.14 c (0.31)	-0.08 c (0.13)	-3.64 b (3.92)	-0.02 b (0.82)	-0.34 a (0.38)	0.02 b (0.11)
Total	0.35 (0.83)		0.73 (1.98)	-0.88 (1.22)	0.20 (0.47)	-0.13 (0.16)	-3.21 (3.67)	0.06 (0.74)	-0.43 (0.58)	0.04 (0.13)
Broadleaves	0.79 (0.96)	RCP8.5	2.11 b (2.20)	3.21 b (2.79)	0.93 a (0.96)	1.37 a (1.13)	-4.32 c (3.14)	-5.48 c (2.42)	-1.30 c (1.11)	-1.05 d (0.73)
Conifers	0.17 (0.71)		3.38 a (1.74)	3.75 a (2.51)	0.37 b (0.45)	0.78 b (0.62)	-5.68 d (3.77)	-6.4 d (3.21)	-0.61 b (0.46)	-0.57 c (0.53)
Total	0.35 (0.83)		3.02 (1.96)	3.60 (2.58)	0.53 (0.68)	0.95 (0.83)	-5.29 (3.63)	-6.11 (3.02)	-0.81 (0.77)	-0.71 (0.63)

Table 2. Growth trends as estimated by the slopes of linear regressions between growth (slopes in $cm^2 \cdot year^{-2}$) or GPP (slopes in g C m^{-2} $year^{-2}$) and year. Mean slopes are shown for observed past growth and for projected growth and GPP for the periods 2010-2050 and 2051-2099. Standard deviations are between parentheses. One-way ANOVA differences between broadleaves and conifers (RCP2.6 and RCP85, i.e. 4 levels) within columns are depicted with different letters.

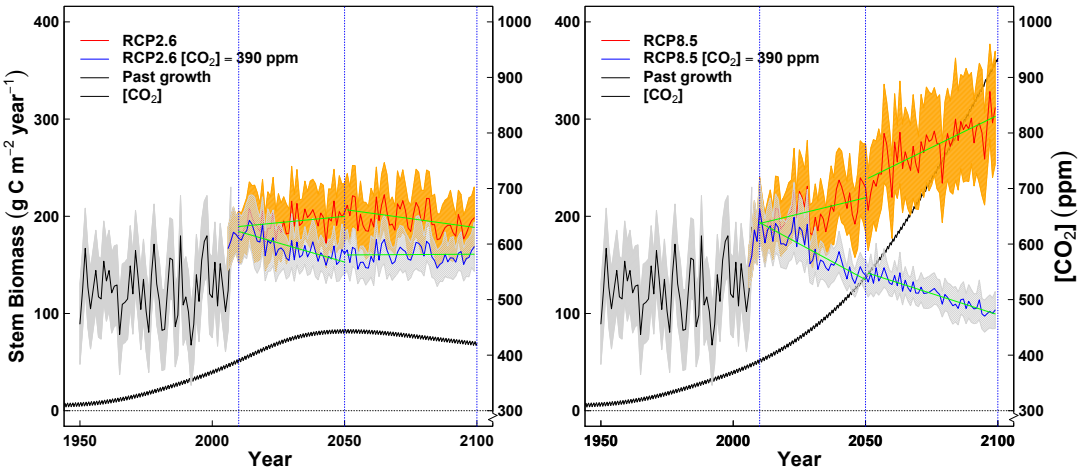

Fig. 4. Example of growth projections at one *Quercus pyrenaica* site (QUPY3 in App.1). Trends (i.e. linear regressions between mean growth and year) for 2010-2050, and 2051-2099 are shown with green lines for the 'fertilization' (red line) and 'non-fertilization' (blue line) scenarios. These trends correspond to the slopes reported in Table 2, Fig. 5 and Fig. 6. Shaded areas behind annual mean growth values ($\hat{y}$; thick black line is mean past growth) correspond to the confidence intervals for the mean calculated as $\hat{y} \pm 1.96 \cdot sd_{\hat{y}}/\sqrt{n}$ ($sd_{\hat{y}}$ is the combined standard deviation of the model estimates and the variability among climatic scenarios; n is sample size). c_a values ($[CO_2]$) corresponding to the two scenarios considered (i.e. RCP2.6, RCP8.5) are shown as thin black lines.

2). GPP projections exhibited steeper trends (both positive and negative) for Mediterranean conifers (all evergreen species), whereas the growth trends were steeper for broadleaves (mostly deciduous) than for conifers (Table 2). An example of a model simulation and how the reported trends (i.e. slopes) were calculated is depicted in Fig. 4. Model simulations yielded the greatest GPP and growth in more mesic sites, as expected (App. 6).

354 According to our projections forest growth would not be much altered when
355 assuming the low emission RCP2.6 scenario with predicted c_a (Fig. 5). Under the c_a
356 pathway from RCP2.6, which reaches the c_a maximum (446 ppm) in 2051, the model
357 simulates a slight increase in growth up to 2050 followed by a slight decrease (Table 2).
358 The resulting overall trend up to 2100 depends on site conditions: most forests exhibited
359 non-significant or reduced trends under RCP2.6 for both c_a scenarios (Fig. 5, 6).
360 However, for the 'non-fertilization' scenario, model simulations suggested significant
361 negative growth trends for some coniferous sites e.g. in Southern France and Eastern
362 Spain (Fig. 6). Therefore the results of the model mostly suggested that forests would
363 acclimate at the regional scale to the climate proposed by RCP2.6. Yet, negative local
364 impacts for some coniferous species would pop up when constraining the carbon
365 fertilization effect.
366 Climate simulations under RCP8.5 forecast a much warmer scenario with less
367 precipitation than RCP2.6 (App. 3). In response, forest growth projections under this
368 scenario showed a different picture to that described for RCP2.6. For the 'non-
369 fertilization' scenario (i.e. constant 390 ppm) future forest growth trends would be
370 negative across all the western Mediterranean. Both conifers and broadleaves would
371 suffer huge decreases in GPP and growth concurrent with the increase in PET expected
372 under RCP8.5. These negative trends were much steeper than those for RCP2.6 (Table
373 2) and in some cases converged towards zero. In contrast, under the coherent c_a pathway
374 (exponential increase in c_a to 935 ppm in 2100) for RCP8.5, the model suggested that
375 plants would not only compensate the more stressing climate but also that growth and
376 GPP would be enhanced across the study region regardless of species (Fig. 6; Table 2).
377 In average RCP8.5 predicts for the studied area in average a +2ºC warmer climate
378 (with c_a = 504 ppm) and a slight MAP reduction by 2050 (App. 3) compared to present

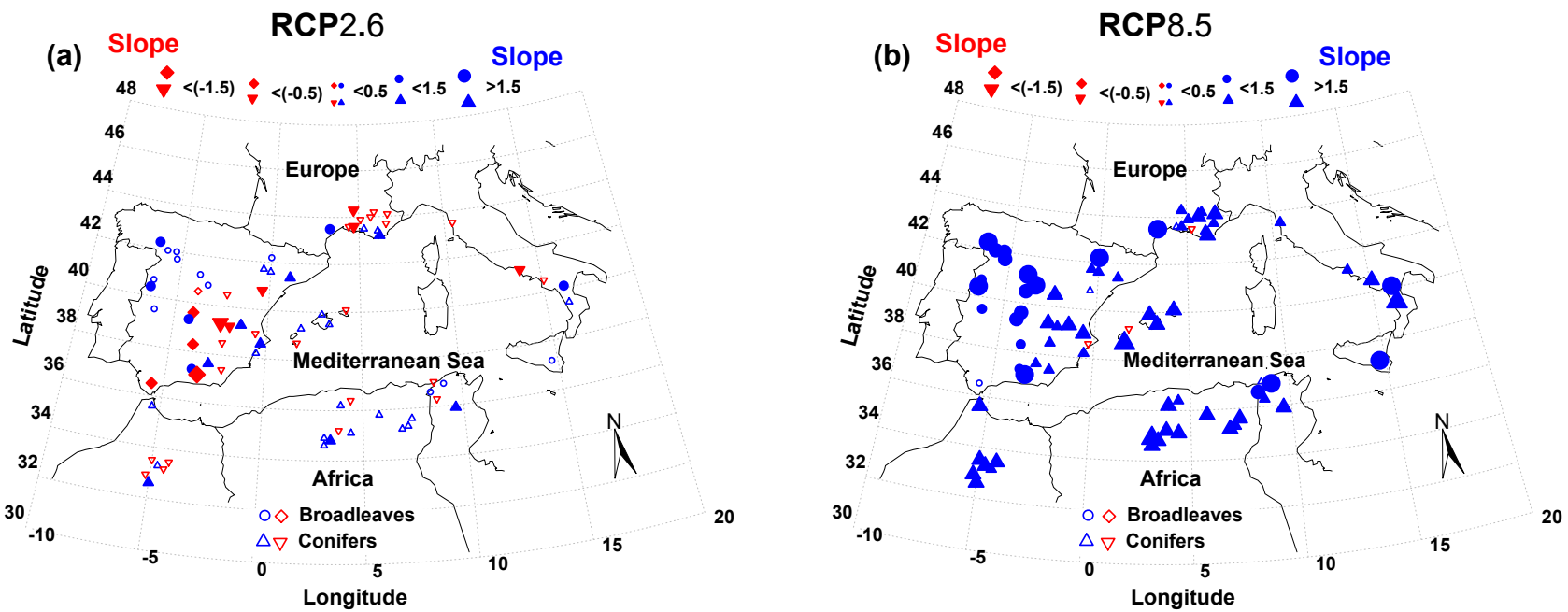

379

380 Fig. 5. Future growth simulations trends using climatic scenarios RCP2.6 (a) and RCP8.5 (b), with predicted (increasing) c_a between 2010 and

381 2099. Trends are estimated as the slopes of the linear regressions between stem biomass growth and year (see Fig. 4). Symbols are scaled as a

382 function of the slope value. Red symbols correspond to negative trends whereas blue symbols to positive trends. Solid symbols correspond to

383 significant trends (α=0.05) whereas empty symbols to non-significant trends.

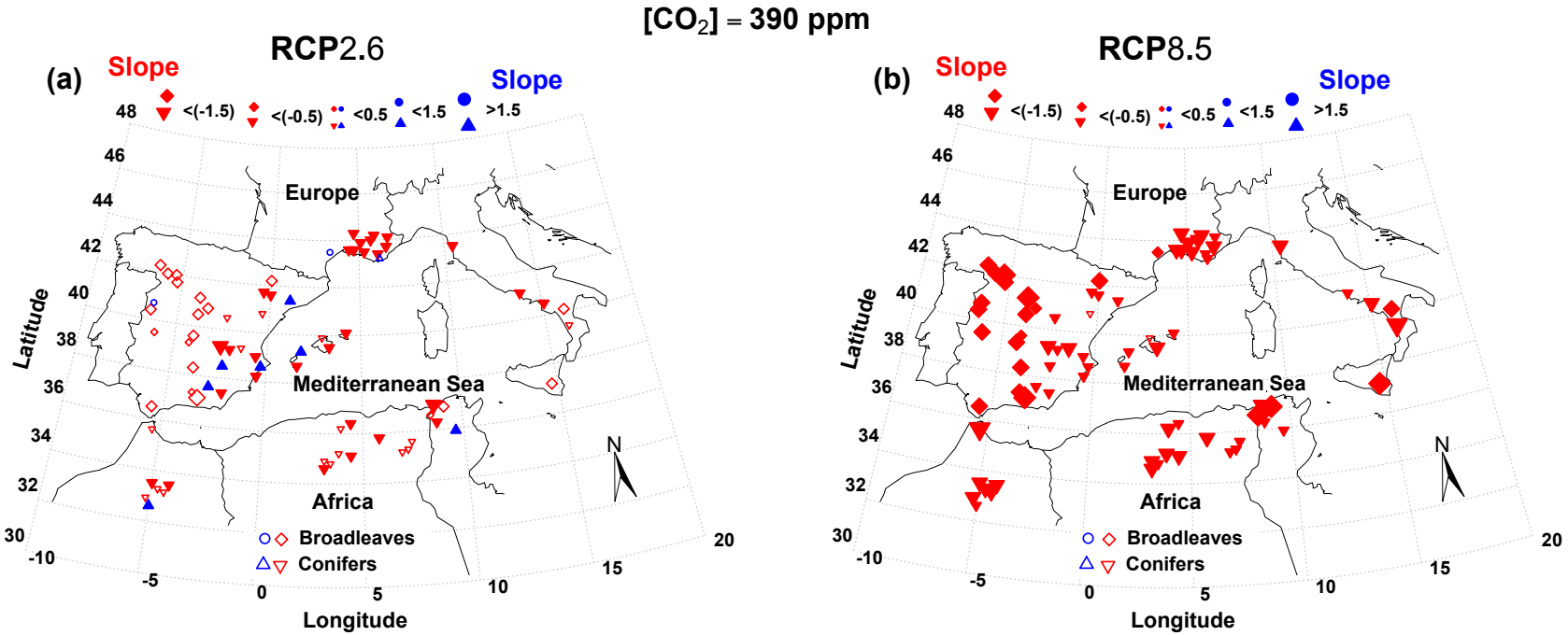

Fig. 6. Future growth simulations trends between 2010 and 2099 using climatic scenarios RCP2.6 (a) and RCP8.5 (b), with constant c_a = 390 ppm. Trends are estimated as the slopes of linear regressions between stem biomass growth and year (see Fig. 4). Symbols are scaled as a function of the slope value. Red symbols correspond to negative trends whereas blue symbols to positive trends. Solid symbols correspond to significant trends (α=0.05) whereas empty symbols to non-significant trends.

values (i.e. +2.8ºC compared to preindustrial levels). This is over the reduction goal in greenhouse emissions for COP21 (http://www.cop21paris.org/) established below +2ºC, which otherwise would be achieved in RCP2.6. Simulations under RCP8.5 suggested a negative impact in growth and GPP of climate unless this was compensated by an exaggerated fertilization effect of eCO_2. The higher the temperature, the more evident and widespread this negative impact would become (Fig. 5, 6; Table 2). In contrast, when allowing fertilization, the greatest positive growth trends (i.e. a greater net fertilization effect) would arise after 2050 with c_a levels >500 ppm (Table 2). Growth trends after 2050 were steeper than those before 2050 for the 'fertilization' scenario (mean difference 0.42, $p<0.001$) but not for the 'non-fertilization' scenario (mean difference 0.09, $p=0.403$). This highlights the larger influence in simulated growth and GPP of eCO_2 (positive) compared to that of expected high temperatures (negative).

Discussion

Forest future in a warmer western Mediterranean region: what is the role of c_a?

Trees can enhance productivity and modify some anatomical and physiological traits (e.g. iWUE) in response to eCO_2 but it is not known how they will perform under future climate and c_a (Medlyn & De Kauwe 2013; Duursma *et al*. 2016; Kelly *et al*. 2016). A positive net effect of eCO_2 on trees can be hampered by the limiting effect of other environmental constraints such as nitrogen (N) availability and water stress (De Kauwe *et al*. 2013; Reichstein *et al*. 2013; Fernández-Martínez *et al*. 2014; Walker *et al*. 2015; Kim *et al*. 2016). A positive feedback of eCO_2, e.g. in leaf area (if a steady-state has not been achieved yet; Körner 2006) and NPP, has been reported under current climate conditions in temperate forests where non-climatic factors such as N availability were limiting (Medlyn *et al*. 2015; Walker *et al*. 2015; Kim *et al*. 2016). In contrast,

414 Duursma *et al*. (2016) did not observe any change in leaf area in response to eCO_2 when
415 leaf area was limited by water availability (i.e. like in our model). Therefore, depending
416 on the most limiting factor, different ecosystems seem to express different responses to
417 eCO_2 under current climatic conditions.

418 As reflected by our model during the observational period (see Gea-Izquierdo *et al*.
419 2015 for iWUE), the effect of recent rising c_a has generally produced an enhancement in
420 iWUE but not in growth rates (e.g. Peñuelas *et al*. 2011; Keenan *et al*. 2013; Saurer *et*
421 *al*. 2014; van der Sleen et al. 2014). Furthermore, studies reporting past growth
422 enhancement within the last 150 years (e.g. at species-specific high-elevation sites) did
423 not consider c_a as the main factor triggering that growth increase (Salzer *et al*. 2009;
424 Gea-Izquierdo & Cañellas 2014). According to our results, most Mediterranean forests
425 would mitigate the optimistic RCP2.6 scenario either with or without C-fertilization.
426 Hence, forests would mostly endure the +2°C warming limit set within the Paris'
427 Agreement (http://www.cop21paris.org/). In contrast, projections under high-emission
428 RCP8.5 would forecast big changes in forest performance. Simulations reflected a very
429 negative impact of climatic conditions under RCP8.5 and a non-fertilization scenario,
430 whereas they suggested a dominant positive effect of eCO_2 at the regional scale
431 (particularly for c_a > 500 ppm) when allowing fertilization even under the very limiting
432 climatic conditions of RCP8.5. The observed positive trends following a Temperature x
433 eCO_2 interaction were not unexpected, because the Farquhar model ensures large direct
434 responses to eCO_2 since Rubisco-limited photosynthesis responds fast to enhanced c_a
435 (Reichstein *et al*. 2013; Friend et al. 2014; Baig *et al*. 2015; Walker *et al*. 2015; Norby
436 *et al*. 2016). Yet, this fertilization effect both for GPP and growth under RCP8.5 looks
437 unrealistic (Körner 2006; Friend et al. 2014; Baig *et al*. 2015; Kelly *et al*. 2016).

438 The future long-term response of forests is uncertain but we expected no positive
439 net effect of eCO_2 on plant growth under very strong water-limitations (van der Molen
440 *et al*. 2011; Girardin *et al*. 2012; Baig *et al*. 2015). Nevertheless, this was only reflected
441 for RCP8.5 by the non-fertilization scenario. Photosynthesis is a saturating function of
442 intercellular CO_2 (Kelly *et al*. 2016) and according to Körner (2006) saturation is
443 expected at levels similar to those of RCP8.5 in 2100 (circa 1000 ppm). Likely, the
444 model does not downregulate assimilation enough under high c_a or underestimates the
445 limiting effect of other interacting factors (e.g. light, nutrients, water stress, hydraulics)
446 on e.g. maximum carboxylation. This was addressed empirically by setting a limit at
447 390 ppm but a more detailed understanding of the physiological processes in relation to
448 eCO_2 would definitely help to improve model forecasts. A global negative response of
449 Mediterranean forests to intense warming unless there is an exaggerated C-fertilization
450 effect is, thus, evident in our results. Importantly, this implies negative consequences
451 for forest performance and means that a positive effect of milder winters (e.g. earlier
452 growing season or enhanced winter assimilation in evergreens) would not counteract the
453 negative effect of longer stressing summers. There is an ample debate on the actual
454 factors causing tree death, but it seems that a combination of interrelated C-related
455 traits, hydraulically-related features and climate-related impacts of biotic agents should
456 govern the forest decline and mortality processes (Sala *et al*. 2012; McDowell *et al*.
457 2013; Aguadé *et al*. 2015; Anderegg *et al*. 2015). Regardless of the final causal factor/s,
458 steep negative growth trends like those under RCP8.5 and no-fertilization strongly
459 suggest changes in stand dynamics and composition and ultimately enhanced mortality
460 at some sites (Bigler *et al*. 2006; van der Molen *et al*. 2011; Gea-Izquierdo *et al*. 2014).
461
462 *Forest growth projections under climate change and eCO_2: utilities and uncertainties*

463 Models need continuous refinement to achieve robustness, reliability and realism
464 (Prentice et al. 2015). Forecasts of tree growth are a valuable tool to understand forest
465 performance under climate change but there are many sources of uncertainty within
466 model performance and data-assimilation that need discussion (Friend et al. 2014).
467 Caveats in models include: (i) current knowledge of the physiological processes; (ii)
468 model implementation and parameterization (including scale-dependent constraints);
469 (iii) uncertainty of model outputs outside the calibration range (Pappas *et al*. 2013;
470 Prentice *et al*. 2015). Additionally, changes in plasticity of functional traits and plant
471 acclimation processes can bias model projections (Muller et al. 2011). We assumed
472 uniformitarianism (i.e. temporal invariance of the modeled relationships) in model
473 projections but it could be that threshold related responses arise after the calibration
474 boundaries are surpassed. In this sense (iii) is minimized by explicitly modeling
475 processes but not eliminated as a result of (i) and (ii). Despite inherent limitations in
476 models and observational data (Babst *et al*. 2014), by using data-assimilation we
477 maximized the likelihood of getting unbiased past long-term trends to increase
478 reliability of growth projections (Peng *et al*. 2011; Medlyn *et al*. 2015). Forest
479 productivity was analyzed assuming present steady-state stand conditions (e.g.
480 composition, leaf area, root mass) constrained by water stress (Körner 2006). This could
481 bias the analysis of forest dynamics (Körner 2003; Friend et al. 2014; Pappas *et al*.
482 2015), particularly for mixed stands (Pappas et al. 2013). However, our aim was to
483 analyze performance of the present stands under future environmental conditions, with
484 emphasis on species long-term trends. Changes in inter-species dynamics are away from
485 the scope of our analysis and need to be studied complementary.

486 The model does not include nutrient dynamics but focuses on the water and carbon
487 cycles and the effect of water stress at different functional levels. This is because

488 nutrient availability is generally considered secondary in Mediterranean ecosystems
489 compared to water stress, which in addition is expected to increase in the future (Giorgi
490 & Lionello 2008; García-Ruiz *et al*. 2011; IPCC 2014). Thus, the limiting effect of
491 factors such as availability of N, P, or hydraulic constraints could invalidate a C
492 fertilization effect on net growth under eCO_2 (Körner 2006; Norby *et al*. 2010; Fatichi
493 *et al*. 2014; Fernández *et al*. 2014; Friend *et al*. 2014; Baig *et al*. 2015). Our model is
494 simpler than ecosystem models including nutrient and stand dynamics (e.g. Reichstein
495 *et al*. 2013; Walker *et al*. 2015). However, our scale is finer (stand, species-specific
496 compared to PFTs) and, most important, it is driven by actual growth data to ensure
497 unbiased estimation of short- and long-term trends. Other factors such as differences in
498 carry-over effects between conifers and broadleaves, changes in species composition
499 and demography, competition and tree-related traits such as ontogeny and size, partly
500 modulate the forest response to climate (van der Molen *et al*. 2011). However, long-
501 term stand productivity seems to change slightly under moderate disturbances such as
502 those produced by silvicultural treatments or insect infestation (Vesala *et al*. 2005;
503 Amiro *et al*. 2010). Therefore, we believe that climate effects are dominant and the
504 reported long-term trends are robust in relation to variability within these other factors,
505 which would affect mostly in the short-term. The model fit reported was in the range of
506 that in similar studies (Misson 2004; Li *et al*. 2014; Gea-Izquierdo *et al*. 2015; Girardin
507 *et al*. 2016). Different goodness-of-fit at different sites could result on differences in
508 model performance. However, in App. 7A we show how variability in R^2 did not
509 influence the estimated trends (future projections). Particularly, when the trees exhibited
510 long-term trends in the past (observational period), these showed a very high agreement
511 with the modeled growth trends (App. 7B; Table 1). As mentioned, the robustness of
512 our approach relies on the spatial (regional) scale where the model was applied, which

513 expands model implementation at a broader scale than that where it was previously
514 applied (Misson et al. 2004; Gaucherel et al. 2008; Gea-Izquierdo et al. 2015).

515 Model simulations can be improved by better addressing the influence of CO_2 on
516 variability of different plant traits (Kattge *et al*. 2011; Atkin *et al*. 2015; Pappas *et al*.
517 2016). Leaf photosynthesis is negatively affected by drought through several
518 mechanisms including changes in stomatal and mesophyll conductance or reductions in
519 biochemical efficiency (Flexas *et al*. 2005). Both photosynthesis and stomatal
520 conductance were modeled as direct functions of CO_2. However, warming and
521 increasing water stress in relation to eCO_2 could differently affect autotrophic
522 respiration and photosynthetic capacity, or enhance photorespiration more than
523 photosynthesis (Baig *et al*. 2015; Girardin *et al*. 2016; Rowland *et al*. 2015; Varone &
524 Gratani 2015). Our model takes into account the short-term acclimation of leaf
525 photosynthesis and stomatal conductance to CO_2, while respiration is set as a function
526 of temperature and GPP (Gea-Izquierdo *et al*. 2015). Different sources of interspecific
527 variability under eCO_2 in autotrophic respiration not explained by models (Atkin *et al*.
528 2015) or other factors such as species-specific variability in J_{max}/Vc_{max} could partly
529 impair our results. Trees modify other traits such as leaf area and sapwood area to
530 withstand xericity (Breda *et al*. 2006; Martin-StPaul *et al*. 2013; Duursma *et al*. 2016;
531 Kelly *et al*. 2016). In our model, intra-annual, inter-annual and long-term structural
532 acclimation of leaf area and allocation rules rely on climate and SWC but not on CO_2.
533 Thus, addressing the influence of CO_2 on leaf area dynamics by setting SLA and
534 allocation rules also as functions of CO_2 could also help to better assess whether the
535 reported fertilization effect is unrealistic (Duursma *et al*. 2016; Medlyn *et al*. 2015).

536 In summary, modeled forest growth reflected the observed absence of an overall net
537 positive effect of enhanced c_a under increased temperatures (i.e. PET) in the recent past.

According to model projections, western Mediterranean forests would mostly mitigate the negative effect of a climate remaining below the maximum warming levels (+2ºC) agreed in COP21 (i.e. scenario RCP2.6) but the situation would be very different above those levels (as represented by RCP8.5). Our results suggest that fertilization could override the negative effect of stressing climatic conditions under high-emission RCP8.5 but this fertilization effect of eCO_2 looks unrealistic according to the literature, being most likely a result of miss-performance of models way above the calibration c_a levels. Consequently, simulations precluding fertilization under high-emission scenarios show very negative forest performance at the regional scale in the future for both conifers and broadleaves. Our results suggest that western Mediterranean forests would not resist the stressing conditions of a much warmer climate unless species exhibited an exaggerated C fertilization effect. It is necessary to include c_a variability in forest models but it is not enough. We still need a better understanding of the physiological processes governing the capacity of acclimation of different plant traits (e.g. V_{cmax}) to the interaction between water stress, eCO_2 and nutrient availability. In this sense, our simulations precluding a fertilization effect seems more realistic than those allowing fertilization under c_a levels way above those used to calibrate models. Our study provides a comprehensive data-driven analysis of the likely performance of western Mediterranean forests under predicted climate change and c_a. Yet model performance still needs to be refined under high c_a as expected in the future.

Acknowledgements

This study was funded by project AGL2014-61175-JIN of the Spanish Ministry of Economy and Competitiveness and the Labex OT-Med (n° ANR-11-LABEX-0061) from the «Investissements d'Avenir» program of the French National Research Agency

563 through the A*MIDEX project (n° ANR-11-IDEX-0001-02). The climate simulations
564 have been extracted from the CMIP5 site (https://esgf-index1.ceda.ac.uk/projects/esgf-
565 ceda/) and processed with the help of Romain Suarez.

566

567 **References**

568 Aguadé D, Poyatos R, Gómez M, Oliva J, Martínez-Vilalta J (2015) The role of
569 defoliation and root rot pathogen infection in driving the mode of drought-related
570 physiological decline in Scots pine (*Pinus sylvestris* L.). Tree Physiology, **35**, 229–
571 242.

572 Allen RG, Pereira LS, Raes D, Smith M (1998) Crop Evapotranspiration – Guidelines
573 for Computing Crop Water Requirements, FAO Irrigation and Drainage Paper 56,
574 FAO, 1998, ISBN 92-5-104219-5.

575 Amiro BD, Barr AG, Barr JG *et al*. (2010) Ecosystem carbon dioxide fluxes after
576 disturbance in forests of North America. Journal of Geophysical Research:
577 Biogeosciences, **115,** G00K02, doi:*10.1029/2010JG001390*.

578 Anderegg WRL, Schwalm C, Biondi F *et al*. (2015) Pervasive drought legacies in forest
579 ecosystems and their implications for carbon cycle models. Science, **1**, 528–532.

580 Atkin OK, Bloomfield KJ, Reich PB *et al*. (2015) Global variability in leaf respiration
581 in relation to climate, plant functional types and leaf traits. New Phytologist, **206**,
582 614–636.

583 Babst F, Alexander MR, Szejner P *et al*. (2014) A tree-ring perspective on the terrestrial
584 carbon cycle. Oecologia, **176**, 307–322.

585 Baig S, Medlyn BE, Mercado LM, Zaehle S (2015) Does the growth response of woody
586 plants to elevated CO_2 increase with temperature? A model-oriented meta-analysis.
587 Global Change Biology, **21**, 4303–4319.

588 Baldocchi DD, Ma SY, Rambal S *et al*. (2010) On the differential advantages of
589 evergreenness and deciduousness in mediterranean oak woodlands: a flux
590 perspective. Ecological Applications, **20**, 1583–1597.
591 Battipaglia G, Saurer M, Cherubini P, Calfapietra C, McCarthy HR, Norby RJ, Cotrufo
592 MF (2013) Elevated CO_2 increases tree-level intrinsic water use efficiency:
593 insights from carbon and oxygen isotope analyses in tree rings across three forest
594 FACE sites. New Phytologyst, **197**, 544-554.
595 Bigler C, Braker OU, Bugmann H, Dobbertin M, Rigling A (2006) Drought as an
596 inciting mortality factor in Scots pine stands of the Valais, Switzerland.
597 Ecosystems, **9**, 330–343.
598 Breda N, Huc R, Granier A, Dreyer E (2006) Temperate forest trees and stands under
599 severe drought: a review of ecophysiological responses, adaptation processes and
600 long-term consequences. Annals of Forest Science, **63**, 625–644.
601 De Kauwe MG, Medlyn BE, Zaehle S *et al*. (2013) Forest water use and water use
602 efficiency at elevated CO_2: a model-data intercomparison at two contrasting
603 temperate forest FACE sites. Global Change Biology, **19**, 1759–1779.
604 Duursma RA, Gimeno TE, Boer MM, Crous KY, Tjoelker MG, Ellsworth DS (2016)
605 Canopy leaf area of a mature evergreen Eucalyptus woodland does not respond to
606 elevated atmospheric [CO_2] but tracks water availability. Global Change Biology,
607 **22**, 1666-1676.
608 Falge E, Baldocchi D, Tenhunen J *et al*. (2002) Seasonality of ecosystem respiration
609 and gross primary production as derived from FLUXNET measurements.
610 Agricultural and Forest Meteorology, **113**, 53–74.
611 Farquhar GD, von Caemmerer S, Berry JA (1980) A biochemical model of
612 photosynthetic CO_2 assimilation in leaves of C3 species, Planta, **149**, 78–90.

613 Fatichi S, Leuzinger S, Körner C (2014) Moving beyond photosynthesis : from carbon
614 source to sink-driven vegetation modeling. New Phytologist, **201**, 1086–1095.
615 Fatichi S, Pappas C, Ivanov VY (2015) Modeling plant-water interactions: an
616 ecohydrological overview from the cell to the global scale. Wiley Interdisciplinary
617 Reviews Water 3, 327–368.
618 Fernández-Martínez M, Vicca S, Janssens IA et al. (2014) Nutrient availability as the
619 key regulator of global forest carbon balance. Nature Climate Change, **4**, 471–476.
620 Flexas J, Bota J, Galmes J, Medrano H, Ribas-Carbo M (2006) Keeping a positive
621 carbon balance under adverse conditions: responses of photosynthesis and
622 respiration to water stress. Physiologia Plantarum, **127**, 343–352.
623 Friend AD, Lucht W, Rademacher TT et al. (2014) Carbon residence time dominates
624 uncertainty in terrestrial vegetation responses to future climate and atmospheric
625 CO_2. Proceedings of the Natural Academy of Sciences of the United States of
626 America, **111**, 3280–5.
627 Fritts HC (1976) Tree Rings and Climate. Blackburn Press, p. 567.
628 García-Ruiz JM, Ignacio Lopez-Moreno J, Vicente-Serrano SM, Lasanta-Martinez T,
629 Begueria S (2011) Mediterranean water resources in a global change scenario.
630 Earth-Science Reviews, **105**, 121–139.
631 Gaucherel C, Guiot J, Misson L (2008) Evolution of the potential distribution area of
632 french mediterranean forests under global warming. Biogeosciences, **5**, 1493–
633 1504.
634 Gea-Izquierdo G, Cañellas I. (2014) Contrasting instability in growth trends of
635 Mediterranean oaks at opposite distributional limits. Ecosystems, **17**, 228-241.

636 Gea-Izquierdo G, Viguera B, Cabrera M, Cañellas I (2014) Drought induced decline
637 could portend widespread pine mortality at the xeric ecotone in managed
638 mediterranean pine-oak woodlands. Forest Ecology and Management, **320**, 70–82.
639 Gea-Izquierdo G, Guibal F, Joffre R, Ourcival J-M, Simioni G, Guiot J. (2015)
640 Modelling the climatic drivers determining photosynthesis and carbon allocation in
641 evergreen Mediterranean forests using multiproxy long time series.
642 Biogeosciences, **12**, 3695-3712.
643 Giorgi F, Lionello P (2008) Climate change projections for the Mediterranean region.
644 Global and Planetary Change, **63**, 90–104.
645 Girardin MP, Bernier PY, Raulier F, Tardif JC, Conciatori F, Guo XJ (2012) Testing for
646 a CO_2 fertilization effect on growth of Canadian boreal forests. Journal of
647 Geophysical Research-Biogeosciences, **116**, G01012, doi:10.1029/2010JG001287.
648 Girardin MP, Hogg EH, Bernier PY, Kurz WA, Guo XJ, Cyr G (2016) Negative
649 impacts of high temperatures on growth of black spruce forests intensify with the
650 anticipated climate warming. Global Change Biology, **22**, 627–643.
651 Guiot J, Boucher E, Gea-Izquierdo G (2014) Process models and model-data fusion in
652 dendroecology. Frontiers in Ecology and Evolution, **2**, 1–12.
653 Herrera S, Gutierrez JM, Ancell R, Pons MR, Frias MD, Fernandez J (2012)
654 Development and Analysis of a 50 year high-resolution daily gridded precipitation
655 dataset over Spain (Spain02). International Journal of Climatology, **32**, 74-85.
656 IPCC (2014) Climate Change 2014: Synthesis Report. Contribution of Working Groups
657 I, II and III to the Fifth Assessment Report of the Intergovernmental Panel on
658 Climate Change [Core Writing Team, R.K. Pachauri and L.A. Meyer (eds.)].
659 IPCC, Geneva, Switzerland, 151 pp.

660 Kattge J, Díaz S, Lavorel S *et al*. (2011) TRY - a global database of plant traits. Global
661 Change Biology, **17**, 2905–2935.
662 Keenan TF, Hollinger DY, Bohrer G, Dragoni D, Munger JW, Schmid HP, Richardson
663 AD (2013) Increase in forest water-use efficiency as atmospheric carbon dioxide
664 concentrations rise. Nature, **499**, 324–7.
665 Kelly JWG, Duursma RA, Atwell BJ, Tissue DT, Medlyn BE (2016) Drought x CO_2
666 interactions in trees: A test of the low-intercellular CO_2 concentration (Ci)
667 mechanism. New Phytologist, **209**, 1600–1612.
668 Kim D, Oren R, Qian SS (2016) Response to CO_2 enrichment of understory vegetation
669 in the shade of forests. Global Change Biology, **22**, 944–956.
670 Körner (2003) Slow in, rapid out - Carbon flux studies and Kyoto targets. Science, 300,
671 1242–1243 ST – Slow in, rapid out – Carbon flux s.
672 Körner C (2006) Plant CO_2 responses: an issue of definition , time and resource supply.
673 New Phytologist, **172**, 393–411.
674 Legendre P, Legendre L (1998) Numerical Ecology. 853 pp. Elsevier, Amsterdam.
675 Leuning R (1995) A critical appraisal of a combined stomatal- photosynthesis model for
676 C3 plants. Plant, Cell & Environment, **18**, 339–355.
677 Li G, Harrison SP, Prentice IC, Falster D (2014) Simulation of tree ring-widths with a
678 model for primary production, carbon allocation and growth. Biogeosciences, **11**,
679 6711–6724.
680 Luyssaert S, Inglima I, Jung M *et al*. (2007) CO_2 balance of boreal, temperate, and
681 tropical forests derived from a global database. *Global Change Biology*, **13**, 2509–
682 2537.
683 Martin-Stpaul NK, Limousin J-M, Vogt-Schilb H, Rodríguez-Calcerrada J, Rambal S,
684 Longepierre D, Misson L (2013) The temporal response to drought in a

685 Mediterranean evergreen tree: comparing a regional precipitation gradient and a
686 throughfall exclusion experiment. Global change biology, **19**, 2413–26.
687 McDowell NG, Fisher RA, Xu C *et al*. (2013) Evaluating theories of drought-induced
688 vegetation mortality using a multimodel – experiment framework. New
689 Phytologist, **200**, 304–321.
690 Mediavilla S, Garcia-Ciudad a., Garcia-Criado B, Escudero a. (2008) Testing the
691 correlations between leaf life span and leaf structural reinforcement in 13 species
692 of European Mediterranean woody plants. Functional Ecology, **22**, 787–793.
693 Medlyn B, De Kauwe B (2013) Carbon dioxide and water use in forests. *Nature*, **499**,
694 20–22.
695 Medlyn BE, Zaehle S, De Kauwe MG *et al*. (2015) Using ecosystem experiments to
696 improve vegetation models. Nature Climate Change, **5**, 528–534.
697 Misson L (2004) MAIDEN: a model for analyzing ecosystem processes in
698 dendroecology. Canadian Journal of Forest Research, **34**, 874–887.
699 Montwé D, Isaac-Renton M, Hamann A, Spiecker H (2016) Drought tolerance and
700 growth in populations of a wide-ranging tree species indicate climate change risks
701 for the boreal north. Global Change Biology, **22**, 806–815.
702 Morales P, Sykes MT, Prentice IC *et al*. (2005) Comparing and evaluating process-
703 based ecosystem model predictions of carbon and water fluxes in major European
704 forest biomes. Global Change Biology, **11**, 2211–2233.
705 Muller B, Pantin F, Génard M, Turc O, Freixes S, Piques M, Gibon Y (2011) Water
706 deficits uncouple growth from photosynthesis, increase C content, and modify the
707 relationships between C and growth in sink organs. Journal of Experimental
708 Botany, **62**, 1715–1729.

709 Niinemets U (2010) Responses of forest trees to single and multiple environmental
710 stresses from seedlings to mature plants: Past stress history, stress interactions,
711 tolerance and acclimation. Forest Ecology and Management, **260**, 1623–1639.
712 Norby RJ, Warren JM, Iversen CM, Medlyn BE, McMurtrie RE (2010) CO_2
713 enhancement of forest productivity constrained by limited nitrogen availability.
714 Proceedings of the National Academy of Sciences USA, **107**, 19368–19373.
715 Norby RJ, De Kauwe MG, Domingues TF *et al*. (2016) Model-data synthesis for the
716 next generation of forest free-air CO_2 enrichment (FACE) experiments. New
717 Phytologist, **209**, 17–28.
718 Pappas C, Fatichi S, Leuzinger S, Wolf A, Burlando P (2013) Sensitivity analysis of a
719 process-based ecosystem model: Pinpointing parameterization and structural
720 issues. Journal of Geophysical Research: Biogeosciences, **118**, 505–528.
721 Pappas C, Fatichi S, Rimkus S, Burlando P, Huber M (2015) The role of local scale
722 heterogeneities in terrestrial ecosystem modeling. Journal of Geophysical
723 Research: Biogeosciences, **120**, 341–360.
724 Pappas C, Fatichi S, Burlando P (2016) Modeling terrestrial carbon and water dynamics
725 across climatic gradients: Does plant trait diversity matter? New Phytologist, **209**,
726 137–151.
727 Peng CH, Guiot J, Wu HB, Jiang H, Luo YQ (2011) Integrating models with data in
728 ecology and palaeoecology: advances towards a model-data fusion approach.
729 Ecology Letters, **14**, 522–536.
730 Peñuelas J, Canadell JG, Ogaya R (2011) Increased water-use efficiency during the 20th
731 century did not translate into enhanced tree growth. Global Ecology and
732 Biogeography, **20**, 597–608.

733 Potter KA, Arthur Woods H, Pincebourde S (2013) Microclimatic challenges in global
734 change biology. Global Change Biology, **19**, 2932–2939.
735 Prentice IC, Liang X, Medlyn BE, Wang YP (2015) Reliable, robust and realistic: The
736 three R's of next-generation land-surface modelling. Atmospheric Chemistry and
737 Physics, **15**, 5987–6005.
738 Reichstein M, Bahn M, Ciais P *et al*. (2013) Climate extremes and the carbon cycle.
739 *Nature*, **500**, 287–295.
740 Rowland L, Lobo-do-Vale RL, Christoffersen BO *et al*. (2015) After more than a
741 decade of soil moisture deficit, tropical rainforest trees maintain photosynthetic
742 capacity, despite increased leaf respiration. Global Change Biology, **21**, 4662–
743 4672.
744 Sala A, Woodruff DR, Meinzer FC (2012) Carbon dynamics in trees: feast or famine?
745 Tree physiology, **32**, 764–75.
746 Salzer MG, Hughes MK, Bunn AG, Kipfmueller KF (2009) Recent unprecedented tree-
747 ring growth in bristlecone pine at the highest elevations and possible causes.
748 Proceedings of the National Academy of Sciences USA, **106**, 20348–20353.
749 Saurer M, Spahni R, Frank DC *et al*. (2014) Spatial variability and temporal trends in
750 water-use efficiency of European forests. Global change biology, **20**, 3700–3712.
751 Schaefer K, Schwalm CR, Williams C *et al*. (2012) A model-data comparison of gross
752 primary productivity: Results from the North American Carbon Program site
753 synthesis. Journal of Geophysical Research, **117**, G03010,
754 doi:10.1029/2012JG001960.
755 Sheffield J, Goteti G, Wood EF (2006) Development of a 50-yr high-resolution global
756 dataset of meteorological forcings for land surface modeling. Journal of Climate,
757 **19** (13), 3088-3111.

758 Stephenson NL, Das a J, Condit R *et al*. (2014) Rate of tree carbon accumulation
759 increases continuously with tree size. Nature, **507**, 90–3.
760 van Der Molen MK, Dolman AJ, Ciais P *et al*. (2011) Drought and ecosystem carbon
761 cycling. Agricultural and Forest Meteorology, **151**, 765–773.
762 van der Sleen P, Groenendijk P, Vlam M et al. (2014) No growth stimulation of tropical
763 trees by 150 years of CO_2 fertilization but water-use efficiency increased. Nature
764 Geoscience, **8**, 24–28.
765 van Vuuren DP, Edmonds J, Kainuma M et al. (2011) The representative concentration
766 pathways: An overview. Climatic Change, **109**, 5–31.
767 Varone L, Gratani L (2015) Leaf respiration responsiveness to induced water stress in
768 Mediterranean species. Environmental and Experimental Botany, **109**, 141–150.
769 Vesala T, Suni T, Rannik Ü *et al*. (2005) Effect of thinning on surface fluxes in a
770 boreal forest. Global Biogeochemical Cycles, **19**, 1–11.
771 Walker AP, Zaehle S, Medlyn BE *et al*. (2015) Predicting long-term carbon
772 sequestration in response to CO_2 enrichment: How and why do current ecosystem
773 models differ? Global Biogeochemical Cycles, **29**, 476–495.

774 App. 1. List of chronologies used and their source. Lat=latitude; Long=longitude; Altit=altitude; MAP = mean annual precipitation; MAT= mean

775 annual temperature (ºC); PET_{pm}=Penman-Monteith annual evapotranspiration; P=annual precipitation.

#	Site	Species	Country	Lat (º)	Long (º)	Altit (m)	MAP (mm)	MAT (ºC)	PET_{pm} (mm)	P-PET (mm)	P/PET	Source
1	QUPY2			42.2	-6.7	1300	985	9.65	962.4	22.6	1.02	
2	QUPY3			41.9	-6.2	760	453.9	12.3	1108.9	-655.0	0.41	
3	QUPY4			40.3	-6.8	900	1135.7	14.1	1213.3	-77.6	0.94	
4	QUPY5			40.7	-3.7	1300	580	10.1	1017.0	-437.0	0.57	
6	QUPY7	*Quercus pyrenaica* Willd.	Spain	39.5	-4.3	900	496.5	14.3	1228.9	-732.4	0.40	Gea-Izquierdo *et al*. (2014)
6	QUPY8			38.2	-4.1	890	474	15.0	1356.4	-882.4	0.35	
7	QUPY9			37.2	-4.0	1486	509.8	11.3	1164.8	-655.0	0.44	
8	QUPY10			37.0	-3.7	1550	619.3	9.8	984.5	-365.2	0.63	
9	QUPY11			40.8	-4.2	1056	599.9	10.1	1001.8	-401.9	0.6	
10	QUIL1			41.6	-5.6	740	433.8	12.5	1139.7	-705.9	0.38	
11	QUIL2			40.6	-6.7	700	562.6	12.9	1220.6	-658.0	0.46	
12	QUIL3	*Quercus ilex* L.	Spain	40.4	-4.2	600	516.6	13.3	1169.5	-652.9	0.44	Gea-Izquierdo *et al*. (2011)
13	QUIL4			39.4	-6.4	390	544.1	16.1	1269.4	-725.3	0.43	
14	QUIL5			43.2	3.0	270	1009.1	12.8	1001.5	7.6	1.01	
15	QUFG1			41.9	-5.7	680	453.9	12.3	1107.8	-653.9	0.41	Gea-Izquierdo (Unpublished data)
16	QUFG2	*Quercus faginea* Lam.	Spain	39.2	-4.5	900	496.5	14.3	1231.7	-735.2	0.40	
17	QUFG3			41.5	-0.3	550	326.1	15.3	1272.3	-946.2	0.26	https://www.ncdc.noaa.gov/paleo/study/10475
18	QUPU1	*Quercus pubescens* Willd.	Italy	37.1	14.4	430	537.1	15.8	964.2	-427.1	0.56	Garfi (2000)
19	QUCE1	*Quercus cerris* L.	Italy	40.4	15.8	590	767.3	11.2	878.5	-111.2	0.87	Battipaglia (unpublished data)
20	QUCA1	*Quercus canariensis* Willd.	Spain	36.4	-5.9	330	988.4	16.1	1195.4	-207.0	0.83	Gea-Izquierdo *et al*. (2010)
21	QUCA5			36.8	8.8	758	649.3	16.5	1319	-669.7	0.49	

22	QUCA6			36.5	8.1	760	625.2	15.9	1338.8	-713.6	0.47	
23	PINI2	*Pinus nigra* J.F. Arnold	Algeria	36.3	4.1	1560	580	14.8	1201.0	-621.0	0.48	Touchan *et al*. (2011)
24	PINI5	*Pinus heldreichi* H.Christ	Italy	39.3	15.9	1430	806.1	12.4	901.1	-95.0	0.89	https://dendrodb.eccorev.fr/framedb.htm
25	PIPI2	*Pinus pinaster* Ait.	Morocco	35.5	-5.7	900	611.3	16.4	1156.4	-545.1	0.53	Touchan *et al*. (2011)
26	PIPN1	*Pinus pinea* L.	Spain	40.4	-2.6	1055	443.3	11.4	1217.1	-773.8	0.36	https://www.ncdc.noaa.gov/paleo/study/2863
27	PIPN2			39.1	-1.7	705	379.8	14.0	1269.4	-889.6	0.30	https://www.ncdc.noaa.gov/paleo/study/2866
28	PIPN3			39.2	-2.3	720	264.3	14.1	1330.4	-1066.1	0.20	https://www.ncdc.noaa.gov/paleo/study/2867
29	PIPN4			39.2	-2.8	700	343.3	14.5	1347.4	-1004.1	0.25	https://www.ncdc.noaa.gov/paleo/study/2865
30	PIPN8		Italy	43.4	10.2	10	962.1	15.3	1019.4	-57.3	0.94	https://www.ncdc.noaa.gov/paleo/study/16755
31	PIPN9			41.0	13.6	9	571.8	17.7	974.1	-402.3	0.59	Battipaglia *et al*. (2016)
32	PIHA1	*Pinus halepensis* Mill.	France	43.1	5.9	420	645.9	14.7	1201.2	-555.3	0.54	Gea-Izquierdo *et al*. (2015)
33	PIHA2		Tunisia	36.9	8.3	23	630.3	18.7	1283.0	-652.7	0.49	Gea-Izquierdo (unpublished data)
34	PIHA3			36.2	8.4	950	619.8	15.1	1297.7	-677.9	0.48	Touchan *et al*. (2011)
35	PIHA4			35.8	9.3	800	542.3	14.7	1322.1	-779.8	0.41	
36	PIHA5		Algeria	34.8	2.8	1380	349.6	14.5	1315.3	-965.7	0.27	Safar (1994), Safar *et al*. (1992)
37	PIHA8			35.2	6.9	1300	380.8	14.6	1330.3	-949.5	0.29	
38	PIHA9			35.7	5.5	1200	431.2	15.6	1292.6	-861.4	0.33	
39	PIHA10			35.3	7.1	1650	380.8	14.6	1333.9	-953.1	0.29	
40	PIHA11			35.0	4.1	1100	390.2	15.6	1304.3	-914.1	0.30	
41	PIHA12			35.1	3.5	1060	417.2	15.4	1304.8	-887.6	0.32	
42	PIHA13			34.7	3.1	1410	350.8	14.3	1305.5	-954.7	0.27	
43	PIHA14			34.7	2.8	1350	350.8	14.3	1306.5	-955.7	0.27	
44	PIHA15			35.1	6.6	1450	380.8	14.6	1333.1	-952.3	0.29	
45	PIHA16		France	44.1	5.6	600	845.3	11.4	916.2	-70.9	0.92	Nicault (1999)
46	PIHA17			43.5	4.4	190	743.9	14.0	1029.2	-285.3	0.72	
47	PIHA18			43.8	4.8	330	788.9	13.2	1004.1	-215.2	0.79	
48	PIHA19			43.4	6.3	300	742.4	13.2	973.0	-230.6	0.76	

49	PIHA20			43.2	5.8	200	713.2	14.6	1015.3	-302.1	0.70	
50	PIHA21			43.7	5.4	170	816.3	11.8	944.8	-128.5	0.86	
51	PIHA22			44.0	6.4	600	1073.5	9.4	816.0	257.5	1.32	
52	PIHA23			43.4	5.0	150	749.1	13.6	986.4	-237.3	0.76	
53	PIHA28			44.2	4.4	350	888	12.2	966.6	-78.6	0.92	
54	PIHA31			43.8	4.1	300	743.6	14.2	1023.0	-279.4	0.73	
55	PIHA32			38.6	-2.6	1000	350.6	14.7	1203.4	-852.8	0.29	
56	PIHA34			37.3	-2.5	1280	287.6	14.7	1311.1	-1023.5	0.22	
57	PIHA35			38.9	-0.9	800	333.7	13.8	1270.0	-936.3	0.26	
58	PIHA36			40.8	-0.7	850	453.3	13.7	1152.7	-699.4	0.39	
59	PIHA37			38.1	-0.8	10	276.2	18.0	998.5	-722.3	0.28	
60	PIHA38			38.5	-0.6	900	380.1	14.2	1194.3	-814.2	0.32	
61	PIHA39			37.5	-3.2	1150	380.6	12.8	1362.8	-982.2	0.28	
62	PIHA40		Spain	41.6	-0.3	500	335.9	14.4	1203.3	-867.4	0.28	Ribas (2006)
63	PIHA41			41.3	0.8	750	304	14.2	1197.8	-893.8	0.25	
64	PIHA42			41.8	-0.7	350	310.2	14.2	1194.5	-884.3	0.26	
65	PIHA43			38.7	1.3	80	362.4	18.2	1177.3	-814.9	0.31	
66	PIHA44			40.0	3.9	0	486.9	16.7	1071.7	-584.8	0.45	
67	PIHA45			39.4	3.0	250	430.5	17.9	1080.0	-649.5	0.4	
68	PIHA46			39.8	2.6	700	548.7	14.3	1228.7	-680	0.45	
69	PIHA47			39.1	1.5	175	327.6	17.1	1303.5	-975.9	0.25	
70	PIHA48		Italy	40.3	14.8	8	711.5	15.1	1000.7	-289.2	0.71	Battipaglia *et al*. (2014)
71	CEAT1			32.2	-5.5	1920	483	9.9	1255.1	-772.1	0.38	Touchan *et al*. (2011)
72	CEAT2			33.1	-4.5	2180	526.5	15.2	1266.8	-740.3	0.42	
73	CEAT3	*Cedrus atlantica* (Endl.) Manetti ex Carrière	Morocco	32.3	-5.3	2100	463.7	12.2	1339.1	-875.4	0.35	Esper *et al*. (2007)
74	CEAT4			33.2	-5.3	1830	539.4	10.5	1213.3	-673.9	0.44	
75	CEAT5			32.6	-5.0	2200	492.2	13.5	1360.5	-868.3	0.36	

76	CEAT6		32.6	-4.7	2200	492.2	13.5	1360.5	-868.3	0.36	
77	CEAT7	Algeria	36.3	3.6	1520	576.1	14.7	1196.2	-620.1	0.50	Touchan *et al*. (2011)

776

777 **References**

778 Battipaglia G, Strumia S, Esposito A, Giuditta E, Sirignano C, Altieri S, Rutigliano FA (2014) The effects of prescribed burning on *Pinus*
779 *halepensis* Mill. as revealed by dendrochronological and isotopic analyses. *Forest Ecology and Management*, **334**, 201-208.

780 Battipaglia G, Savi T, Ascoli D, Castagneri D, Esposito A, Mayr S, Nardini A. (2016). Effects of prescribed burning on ecophysiological,
781 anatomical and stem hydraulic properties in *Pinus pinea* L. *Tree physiology* (in press)

782 Esper J, Frank DC, Büntgen U, Verstege A, Luterbacher J, Xoplaki E (2007) Long-term drought severity variations in Morocco. Geophysical
783 Research Letters 34, doi: 10.1029/2007GL030844.

784 Garfì, G. (2000). Climatic signal in tree-rings of *Quercus pubescens* and Celtis australis in South-eastern Sicily. Dendrochronologia 18, 41-51.

785 Gea-Izquierdo G, Cherubini P, Cañellas I. 2011. Tree-rings reflect the impact of climate change on *Quercus ilex* L. along a temperature gradient
786 in Spain over the last 100 years. Forest Ecology and Management 262, 1807-1816.

787 Gea-Izquierdo G, Fonti P, Cherubini P, Martín-Benito D, Chaar H, Cañellas I. 2012. Xylem hydraulic adjustment and growth response of
788 *Quercus canariensis* Willd. to climatic variability. Tree Physiology 32, 401-413.

789 Gea-Izquierdo G, Cañellas I. 2014 Contrasting instability in growth trends of Mediterranean oaks at opposite distributional limits. Ecosystems
790 17, 228-241.
791 Nicault A. (1999). Analyse de l'influence du climat sur les variations inter- et intra-annuelles de la croissance radiale du pin d'Alep (*Pinus*
792 *halepensis* Mill.) en Provence calcaire. Thèse de l'Université d'Aix-Marseille III, 254 p.
793 Ribas M. (2006). Dendroecología de *Pinus halepensis* Mill. en Este de la Península Ibérica e Islas Baleares: Sensibilidad y grado de adaptación a
794 las condiciones climáticas. PhD dissertation. University of Barcelona. http://diposit.ub.edu/dspace/handle/2445/35321
795 Safar W. Serre-Bachet, F. & Tessier L. (1992). Les plus vieux pins d'Alep vivants connus. Dendrochronologia, 10, pp. 41-52.
796 Safar W. (1994). Contribution à l'étude dendoécologique du pin d'Alep (*Pinus halepensis* Mill) dans une région semi-aride d'Algérie : l'Atlas
797 Saharien (Ouled Naïl - Aurès - Hodna). Thèse de l'université d'Aix - Marseille III., 215 p.
798 Touchan, R., K.J. Anchukaitis, D.M. Meko, M. Sabir, S. Attalah, and A. Aloui. (2011) Spatiotemporal drought variability in northwestern Africa
799 over the last nine centuries. Climate Dynamics 37, 237-252.

800 App. 2. Model code and Institute of CMIP5 climate simulations included in the study.

801 Crosses indicate when RCP scenarios where selected for a certain Model.

Model	Institute	RCP2.6	RCP8.5
bcc-csm1-1	Beijing Climate Center, China Meteorological Administration	X	X
bcc-csm1-1-m		X	
BNU-ESM	College of Global Change and Earth System Science, Beijing Normal University	X	X
CanESM2	Canadian Centre for Climate modelling, Canada	X	X
CNRM-CM5	Centre National de Recherches Météorologiques / Centre Européen de Recherche et Formation Avancée en Calcul Scientifique, France	X	X
CSIRO-MK3-6-0	Commonwealth Scientific and Industrial Research Organization in collaboration with Queensland Climate Change Centre of Excellence	X	X
EC-EARTH	EC-EARTH consortium	X	X
FGOALS-g2	LASG, Institute of Atmospheric Physics, Chinese Academy of Sciences and CESS,Tsinghua University	X	X
GFDL-CM3	NOAA Geophysical Fluid Dynamics Laboratory, USA	X	X
GFDL-ESM2G		X	X
GFDLESM2M		X	
HadGEM2-ES	Met-Office – Hadley Center, contributed by Instituto Nacional de Pesquisas Espaciais, Spain	X	X
IPSL-CM5A-LR	Institut Pierre-Simon Laplace, France	X	X
IPSL-CM5A-MR		X	X
MIROC-ESM	Japan Agency for Marine-Earth Science and Technology, Atmosphere and Ocean Research Institute (The University of Tokyo), and National MIROC-ESM-CHEM Institute for Environmental Studies	X	X
MIROC-ESM-CHEM		X	X
MIROC5	Atmosphere and Ocean Research Institute (The University of Tokyo), National Institute for MIROC MIROC4h Environmental Studies, and Japan Agency for MIROC5 Marine-Earth Science and Technology	X	X
MPI-ESM-LR	Max-Planck Inst. Für Meteorologie, Germany	X	X
MRI-CGCM3	Meteorological Research Institute, Japan	X	X
NorESM1-M	Norvegian Climate Centre		X
# Simulations		19	18

802

App. 3. Mean daily annual temperature (MAT) and mean annual precipitation (MAP) of the climate model simulations at each of the 77 sites for the RCP 2.6 (a) and RCP 8.5 (b). Shaded areas are confidence intervals at α=0.05 for annual means.

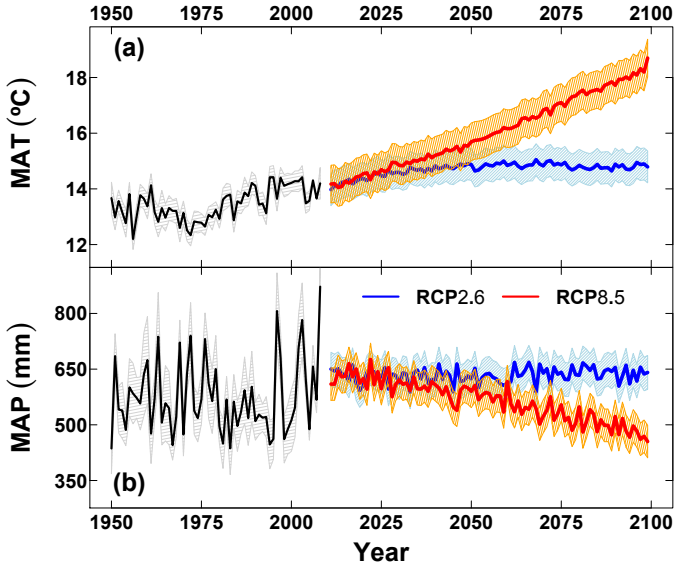

App. 4. Mean values and standard deviations of 7 fitted parameters to the 77 sites.

Parameter	Mean	Standard deviation	Minimum	Maximum
$soil_{ip}$	139.0	96.7	3.1	392.9
p_{3moist}	-0.255	0.211	-0.700	-0.001
p_{3temp}	26.7	77.8	-153.7	181.2
st_{3moist}	-0.226	0.197	-0.699	-0.006
st_{3temp}	4.8	88.2	-167.4	222.0
st_{4sd_moist}	-0.321	0.230	-0.900	-0.009
st_{4temp}	334.9	212.2	49.7	1080.2

App. 5. Distribution of the relationship between GPP and carbon allocation to the stem (i.e. radial growth) as estimated by a linear correlation.

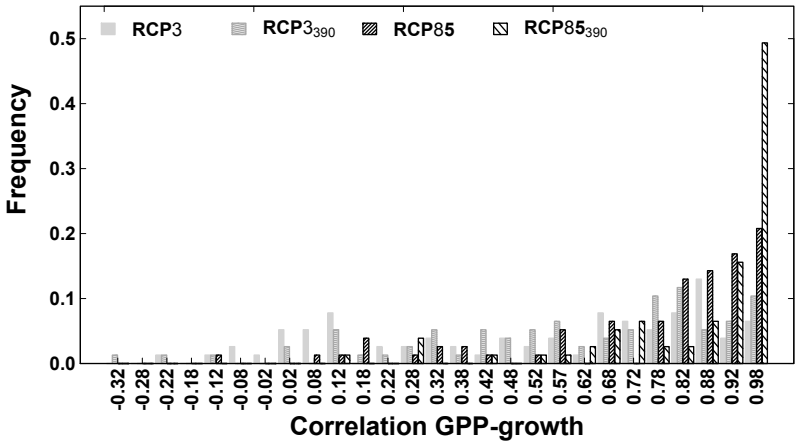

App.6. Mean projected GPP and growth (2010-2100) and site 'Annual precipitation minus Penman-Monteith potential evapotranspiration' (P-PET, in mm) for RCP2.6 and RCP8.5 scenarios: (a) fertilization scenario (i.e. predicted c_a); (b) non-fertilization scenario (i.e. c_a=390 ppm). All relationships (ρ=correlation) are significant at p<0.01.

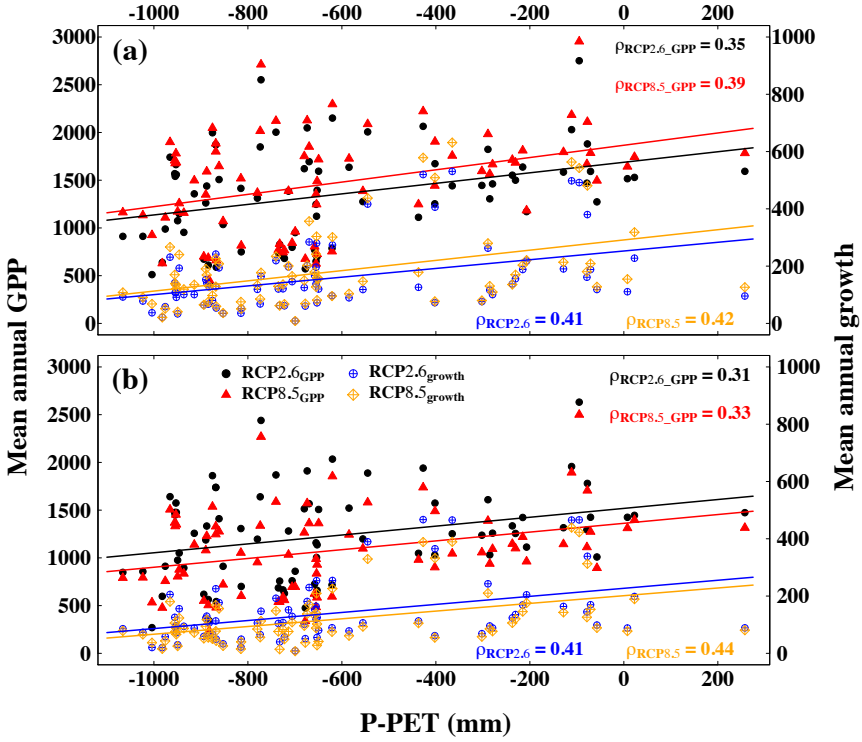

App. 7. In this figure we show two graphs to support the robustness of our modeling approach and the future projections implemented at the regional scale. (A) The coefficient of determination (R^2) is shown as a function of the projected growth trends to demonstrate that there is no relationship between the estimated trends and the calibration R^2. In addition, regardless of R^2, all projections under RCP8.5 are either positive (fertilization, in blue) or negative (non-fertilization, in red), whereas variability in RCP2.6 slopes estimated is independent of the goodness of fit (as estimated by R^2, see (A)). In (B), to illustrate the model capacity to fit the interannual (decadal) growth trends, we show the slopes estimated on past growth observations in function of the r_{low} statistic (correlations between filtered series). r_{low} was greater than 0.7 in 73% of the models fitted (B). Most importantly, r_{low} was greater than 0.6 in all cases when there was a significant past trend (in (B) we highlight those sites where past |slope| ≥ 0.35 $cm^2 \cdot year^{-2}$), which means that the model was able to mimic the long-term growth-trends when trees exhibited some positive or negative trend in the past.